Quantitative Characterization of DNA Films by X-ray Photoelectron Spectroscopy

Dmitri Y. Petrovykh,*,†,‡ Hiromi Kimura-Suda,§ Michael J. Tarlov,§ and Lloyd J. Whitman‡

Physics Department, University of Maryland, College Park, Maryland 20742, Naval Research Laboratory, Washington, D.C. 20375, and National Institute of Standards and Technology, Gaithersburg, Maryland 20899

Received May 29, 2003. In Final Form: September 22, 2003

We describe the use of self-assembled films of thiolated $(dT)_{25}$ single-stranded DNA (ssDNA) on gold as a model system for quantitative characterization of DNA films by X-ray photoelectron spectroscopy (XPS). We evaluate the applicability of a uniform and homogeneous overlayer−substrate model for data analysis, examine model parameters used to describe DNA films (e.g., density and electron attenuation length), and validate the results. The model is used to obtain quantitative composition and coverage information as a function of immobilization time. We find that when the electron attenuation effects are properly included in the XPS data analysis, excellent agreement is obtained with Fourier transform infrared (FTIR) measurements for relative values of the DNA coverage, and the calculated absolute coverage is consistent with a previous radiolabeling study. Based on the effectiveness of the analysis procedure for model $(dT)_{25}$ ssDNA films, it should be generally valid for direct quantitative comparison of DNA films prepared under widely varying conditions.

Introduction

Films of single-stranded DNA (ssDNA) immobilized on surfaces form the basis of a number of important biotechnology applications, including DNA microarrays[1−3] and biosensors.[1,4−6] Relatively little quantitative information is available, however, about the molecular mechanisms of the immobilization processes and the corresponding DNA film structures.[4] In particular, accurate measurement of the surface coverage, a parameter crucial for determination of efficiencies of immobilization and hybridization protocols, is notoriously difficult.[5,7,8] This challenge offsets the otherwise excellent sensitivity of traditional bioanalytical techniques such as fluorescent labeling[3] and newer methods based on electrochemical labels.[9] Although absolute quantification is possible with radiolabeling,[10] its current use is discouraged because of health safety and hazardous waste disposal issues. Labelless film characterization methods such as ellipsometry and surface plasmon resonance[2,7,11,12] provide real-time, in situ results, but possible contributions from nonspecific adsorption complicate the data interpretation. Therefore, label-less methods that provide quantitative and chemically specific information about the DNA films could prove very useful.[7,8] Fortunately, traditional surface analysis spectroscopy methods, such as X-ray photoelectron spectroscopy (XPS), have been developed to provide exactly this type of information. And because DNA films in most current applications are <10 nm thick, XPS can be readily employed to complement traditional biochemical analysis for these samples.[4,13,14]

In this study, we describe how XPS can be used for quantitative characterization of thiolated ssDNA on gold substrates and show that immobilized thymidine homooligonucleotides $[(dT)_{25}-SH]$ form an excellent model film for surface characterization. Chemisorption on gold surfaces via a thiol functional group is a common approach for aqueous DNA immobilization.[5,15] The formation of the ssDNA monolayer in this case is thought to resemble self-assembly of alkanethiols, and the latter process has been extensively studied[16] by many surface science techniques, including XPS.[17−23] In addition to the convenient im-

* To whom correspondence should be addressed. Dmitri Y. Petrovykh, Code 6177, Naval Research Laboratory, Washington, DC 20375-5342. Phone: (202) 404-3381. Fax: (202) 767-3321. E-mail: dmitri.petrovykh@nrl.navy.mil.

† University of Maryland.

‡ Naval Research Laboratory.

§ National Institute of Standards and Technology.

(1) Wang, J. *Nucleic Acids Res.* **2000**, *28*, 3011−3016.

(2) Nelson, B. P.; Grimsrud, T. E.; Liles, M. R.; Goodman, R. M.; Corn, R. M. *Anal. Chem.* **2001**, *73*, 1−7.

(3) Pirrung, M. C. *Angew. Chem., Int. Ed.* **2002**, *41*, 1277−1289.

(4) Kasemo, B. *Surf. Sci.* **2002**, *500*, 656−677.

(5) Tarlov, M. J.; Steel, A. B. In *Biomolecular Films: Design, Function, and Applications*; Rusling, J. F., Ed.; Marcel Dekker: New York, 2003; Vol. 111, pp 545−608.

(6) Homs, W. C. I. *Anal. Lett.* **2002**, *35*, 1875−1894.

(7) Peterson, A. W.; Wolf, L. K.; Georgiadis, R. M. *J. Am. Chem. Soc.* **2002**, *124*, 14601−14607.

(8) Petrovykh, D. Y.; Kimura-Suda, H.; Whitman, L. J.; Tarlov, M. J. *J. Am. Chem. Soc.* **2003**, *125*, 5219−5226.

(9) Anne, A.; Bouchardon, A.; Moiroux, J. *J. Am. Chem. Soc.* **2003**, *125*, 1112−1113.

(10) Steel, A. B.; Levicky, R. L.; Herne, T. M.; Tarlov, M. J. *Biophys. J.* **2000**, *79*, 975−981.

(11) Peterlinz, K. A.; Georgiadis, R. M.; Herne, T. M.; Tarlov, M. J. *J. Am. Chem. Soc.* **1997**, *119*, 3401−3402.

(12) Georgiadis, R.; Peterlinz, K. P.; Peterson, A. W. *J. Am. Chem. Soc.* **2000**, *122*, 3166−3173.

(13) Castner, D. G.; Ratner, B. D. *Surf. Sci.* **2002**, *500*, 28−60.

(14) Fulghum, J. E. *J. Electron Spectrosc. Relat. Phenom.* **1999**, *100*, 331−355.

(15) Herne, T. M.; Tarlov, M. J. *J. Am. Chem. Soc.* **1997**, *119*, 8916−8920.

(16) Schwartz, D. K. *Annu. Rev. Phys. Chem.* **2001**, *52*, 107−137.

(17) Bain, C. D.; Whitesides, G. M. *J. Phys. Chem.* **1989**, *93*, 1670−1673.

(18) Laibinis, P. E.; Whitesides, G. M.; Allara, D. L.; Tao, Y. T.; Parikh, A. N.; Nuzzo, R. G. *J. Am. Chem. Soc.* **1991**, *113*, 7152−7167.

(19) Castner, D. G.; Hinds, K.; Grainger, D. W. *Langmuir* **1996**, *12*, 5083−5086.

(20) Bensebaa, F.; Yu, Z.; Deslandes, Y.; Kruus, E.; Ellis, T. H. *Surf. Sci.* **1998**, *405*, L472−L476.

(21) Rieley, H.; Kendall, G. K.; Zemicael, F. W.; Smith, T. L.; Yang, S. H. *Langmuir* **1998**, *14*, 5147−5153.

(22) Buckel, F.; Effenberger, F.; Yan, C.; Golzhauser, A.; Grunze, M. *Adv. Mater.* **2000**, *12*, 901−905.

10.1021/la034944o CCC: $27.50
Published on Web 12/11/2003

Report Documentation Page

Form Approved
OMB No. 0704-0188

1. REPORT DATE	2. REPORT TYPE	3. DATES COVERED
SEP 2003		**00-00-2003 to 00-00-2003**

4. TITLE AND SUBTITLE	5a. CONTRACT NUMBER
Quantitative Characterization of DNA Films by X-ray Photoelectron Spectroscopy	5b. GRANT NUMBER
	5c. PROGRAM ELEMENT NUMBER
6. AUTHOR(S)	5d. PROJECT NUMBER
	5e. TASK NUMBER
	5f. WORK UNIT NUMBER
7. PERFORMING ORGANIZATION NAME(S) AND ADDRESS(ES) **Naval Research Laboratory,4555 Overlook Avenue SW,Washington,DC,20375**	8. PERFORMING ORGANIZATION REPORT NUMBER
9. SPONSORING/MONITORING AGENCY NAME(S) AND ADDRESS(ES)	10. SPONSOR/MONITOR'S ACRONYM(S)
	11. SPONSOR/MONITOR'S REPORT NUMBER(S)

12. DISTRIBUTION/AVAILABILITY STATEMENT
Approved for public release; distribution unlimited

13. SUPPLEMENTARY NOTES

14. ABSTRACT

15. SUBJECT TERMS

16. SECURITY CLASSIFICATION OF:			17. LIMITATION OF ABSTRACT	18. NUMBER OF PAGES	19a. NAME OF RESPONSIBLE PERSON
a. REPORT **unclassified**	b. ABSTRACT **unclassified**	c. THIS PAGE **unclassified**	**Same as Report (SAR)**	**12**	

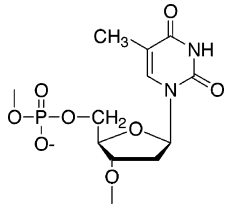

Figure 1. The chemical structure of thymine deoxyribonucleotide (dT). The thymine ring includes two nitrogen atoms in similar bonding configurations that result in a single N 1s XPS core-level peak. The two carbonyl groups provide a unique signature in FTIR.

mobilization chemistry, gold surfaces provide conductive substrates and a number of intense substrate XPS peaks throughout a wide energy range that we use to determine the thickness of the films and to calibrate the binding energy scale. $(dT)_{25}-SH$ has been selected because the chemical structure of a thymidine nucleotide (Figure 1) is simpler than that of the other three nucleotides. In particular, the two nitrogen atoms are in similar environments, and thus comparable chemical shifts and a simple N 1s spectrum are expected and indeed observed. We use the $(dT)_{25}-SH$ films to establish and validate a method to quantitatively analyze DNA films on gold, providing elemental composition data along with both relative and *absolute* values of the ssDNA surface coverage (molecules per unit area).

Materials and Methods

Materials. We used standard 5′ thiol-modified poly$(dT)_{25}$ oligonucleotides [3′-$(dT)_{25}-(CH_2)_6-$SH-5′, from hereon abbreviated $(dT)_{25}-SH$] purchased from Research Genetics. Thiolated probes were used as-received, without removing the protective S-$(CH_2)_6$OH group from the 5′ end. $K_2HPO_4 \cdot 3H_2O$ (Sigma-Aldrich) and 10 × TE (ResGen, 1 × TE; 10 mM Tris−HCl, 1 mM EDTA) were used to prepare buffer solutions for DNA.[24] K_2HPO_4−TE buffer consisted of a 1 M solution of salt and 1 × TE buffer and was adjusted to pH 7 by adding HCl. The 1 μM DNA solution for immobilization experiments was typically prepared by mixing 25 μL of 200 μM $(dT)_{25}-SH$ with 5 mL of buffer. The DNA concentration was confirmed by UV absorption measurements.

Preparation of ssDNA Films. Gold films on single-crystal Si(100) wafers were used as substrates. Prior to deposition of the films, the wafers were cleaned using a "piranha solution" consisting of 70% H_2SO_4 and 30% H_2O_2 (30% H_2O_2 in H_2O). (Note that piranha solution must be handled with care: it is extremely oxidizing, reacts violently with organics, and should only be stored in loosely tightened containers to avoid pressure buildup.) After cleaning, a Cr adhesion layer (20 nm) was deposited by vapor deposition, followed by 200 nm of Au. Each substrate was again cleaned with piranha solution and rinsed thoroughly with deionized water (18.3 MΩ) immediately prior to immobilizing the ssDNA.

Poly$(dT)_{25}$ ssDNA self-assembled monolayers were prepared by immersing clean gold substrates (≈2 cm^2) in 1 μM $(dT)_{25}-SH$ solutions (5 mL) at room temperature. We followed the immobilization conditions established in the previous work,[15] which also allowed us to directly compare our results with several quantitative measurements on similar ssDNA films.[10−12,15] The immobilization was performed in K_2HPO_4−TE buffer for immersion times of 1, 5, 15, 30, 60, 120, and 1200 min. Before analysis, each sample was rinsed thoroughly with deionized water and blown dry under flowing nitrogen.

Fourier Transform Infrared (FTIR) Measurements. FTIR absorption spectra were measured with a Digilab FTS7000 series spectrometer with a PIKE Technologies wire grid infrared polarizer (p polarized) and a VeeMax variable angle specular reflectance accessory (reflectance angle, 75°).[24] Spectra (2000−800 cm^{-1}) were collected from 1024 scans at 2 cm^{-1} resolution using a cryogenic mercury cadmium telluride detector. The FTIR measurements were performed on freshly prepared samples prior to XPS characterization.

XPS Measurements. XPS measurements were performed using a commercial XPS system (Thermo VG Scientific Escalab 220i-XL)[24] equipped with a monochromatic Al Kα source, a hemispherical electron energy analyzer (58° angle between monochromator and analyzer), and a magnetic electron lens. The nominal XPS spot size and analyzer field of view were ≤1 mm^2. The reported binding energies (BEs) are based on the analyzer energy calibration (see Appendix for details). No charge compensation was necessary, and no differential charging features were observed (e.g., low BE tails), most likely because we measured sufficiently thin DNA films on grounded conducting substrates.[25] The absolute XPS peak intensities, where indicated, are based on the count rate recorded by the analyzer; this rate however is a synthetic value calculated by the acquisition software based on signals from six detectors. This synthetic value does not exhibit the statistical behavior of signal-to-noise expected for a single-channel analyzer but otherwise does not appear to affect the analysis.

Three types of normal emission angle-integrated scans were carried out for the samples in this study: survey scans from 0 to 1400 eV BE and 100 eV pass energy (PE), survey scans from 0 to 800 eV BE and 50 eV PE, and high-resolution scans with 15−20 eV windows and 20 eV PE. The nominal analyzer contributions to the overall energy resolution were 1.8, 0.9, and 0.36 eV, respectively. The survey scans were primarily used to monitor samples for the presence of contaminants. High-resolution scans were acquired for the Au 4f, 4d, and 4p, O 1s, C 1s, N 1s, and P 2p regions. These scans were used to determine the stoichiometry and coverage for the DNA films. Spectra of the N 1s and P 2p regions were accumulated for 30−60 min, depending on the sample coverage, to obtain an adequate signal-to-noise ratio. Typically, spectra were acquired from three separate spots on each sample, primarily to test the film uniformity. The corresponding calculated coverage values varied by not more than 10% for each of the samples. In a separate test of the effects of the incident X-ray beam, irradiation of a representative sample for over 3 h using 125 W X-ray source power produced less than a 5% variation in the O, N, and P peak intensities. Carbon peaks were the most affected by the beam exposure, consistent with the presence of a coadsorbed hydrocarbon layer. The reference Au signals used to calibrate the attenuation of the XPS signals were measured from gold films cleaned in situ by Ar ion sputtering until C 1s and O 1s signals were no longer detectable.

XPS Peak Fitting. The peaks in the elemental core-level spectra were fit using commercial XPS analysis software.[24,26] A convolution of Lorentzian and Gaussian line shapes was used to fit the individual peaks. A linear combination of Shirley and linear functions was used to model the background, with the corresponding coefficients fit simultaneously with the peaks. In most cases, the full widths at half-maximum (fwhm's) and background parameters converged to consistent values throughout the series without being restricted, but for a few peaks they were fixed based on values for corresponding spectra with the highest signal-to-noise in the series. XPS spectra are presented in all figures in terms of the XPS intensity recorded by the instrument in order to indicate the experimental signal-to-background ratios. For stacked spectra, the intensity axis always corresponds to the top spectrum in a stack.

XPS Results

In Figures 2 and 3, we present, to our knowledge, the first published set of high-resolution XPS data for all four principal elements in an immobilized ssDNA film (N, P, C, and O; H is not observable by XPS).[8] Previous reports

(23) Kawasaki, M.; Sato, T.; Tanaka, T.; Takao, K. *Langmuir* **2000**, *16*, 1719−1728.

(24) Certain vendors and commercial instruments are identified to adequately specify the experimental procedure. In no case does such identification imply endorsement by the National Institute of Standards and Technology or the Naval Research Laboratory.

(25) Tielsch, B. J.; Fulghum, J. E. *Surf. Interface Anal.* **1997**, *25*, 904−912.

(26) Hesse, R.; Chasse, T.; Szargan, R. *Fresenius' J. Anal. Chem.* **1999**, *365*, 48−54.

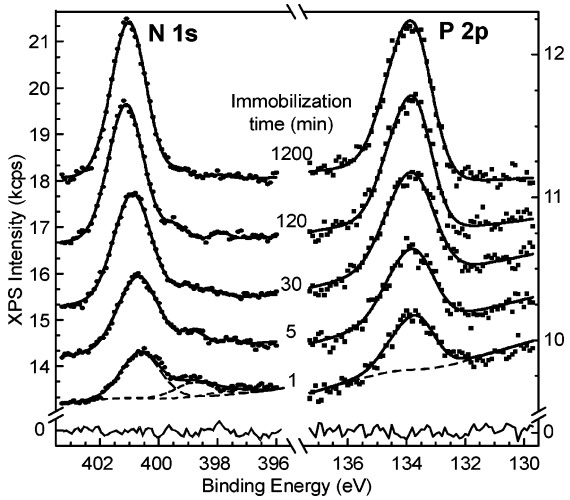

Figure 2. Evolution of the N 1s and P 2p XPS peaks with increasing immobilization time for 1 μM $(dT)_{25}$−SH in 1 M K_2HPO_4−TE buffer. A single N 1s peak between 400.5 and 401.0 eV is characteristic of thymine; the P 2p peak between 133.5 and 134.0 eV is common to all nucleotides. Fitting parameters were chosen for a consistent fit for all samples in the series (filled symbols for raw data, thick lines for total fits, dashed lines for peak components and background).

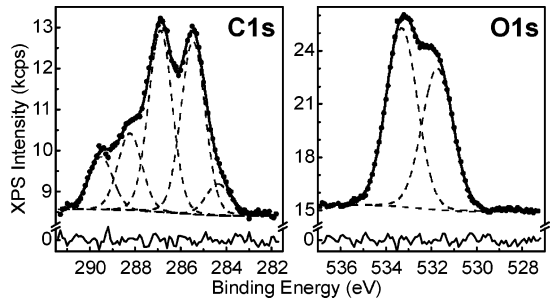

Figure 3. High-resolution XPS spectra of the C 1s and O 1s regions for a ssDNA film after 1200 min of immobilization in 1 μM $(dT)_{25}$−SH (1 M K_2HPO_4−TE buffer). The minimum number of peak components with the same width plus a combination of Shirley and linear backgrounds were chosen for each element to produce random residuals (thin solid lines below fits).

for related systems include two ~30-year-old sets of measurements on adsorbed DNA bases[27,28] and, more recently, limited results for thymine[29] and DNA films.[15,30−33] In contrast to prior work, our spectra were obtained with a high-intensity, monochromatized Al Kα X-ray source that enables superior energy resolution and excellent signal-to-noise, attributes[14] that allow us to perform reliable peak fitting and to observe the detailed evolution of the N 1s spectra with immobilization time (Figure 2). Before proceeding to the more detailed quantitative analysis presented in the following sections, we briefly discuss the general properties representative of a DNA film observed in the data (Figures 2 and 3).

Table 1. Peak Fit Parameters for the Four Major Elements in the $(dT)_{25}$ DNA Film

peak	binding energy (eV)	Lorentzian fwhm[a] (eV)	Gaussian fwhm[a] (eV)	relative intensity
N 1s	401.0	0.1	1.35	0.949
	399.2			0.035
	397.9			0.016
N 1s	400.5	0.1	1.50	0.712
1 min[b]	398.7			0.230
	397.4			0.058
P $2p_{3/2}$	133.7	0.2	1.28	1
P $2p_{1/2}$	134.5[c]			0.5[c]
C 1s	284.4	0.1	1.18	0.062
	285.5			0.337
	286.9			0.349
	288.3			0.150
	289.5			0.102
O 1s	531.7	0.1	1.56	0.443
	533.3			0.557

[a] A convolution of Lorentzian and Gaussian components was assumed for all peak shapes. [b] For the N 1s peaks, parameters for films with the highest and the lowest coverage in the series (after 1200 and 1 min of ssDNA immobilization, respectively) are given (Figure 2). [c] For the P 2p doublet, a spin−orbit splitting of 0.84 eV and a 0.5 intensity ratio have been assumed. The P 2p parameters are given for the 1200 min sample (top spectrum in Figure 2).

The presence of N[15,31] or, to a better extent, N and P together, is an excellent indicator specific to adsorbed DNA[8,30] because their presence is typically unaffected by surface contamination during sample preparation and handling. The base-specific P/N ratio is particularly useful (ideally 1/2 for dT) for checking the film stoichiometry, as discussed in more detail in the next section.

Peak parameters are given in Table 1 corresponding to the fits shown in Figure 2 for N and P and in Figure 3 for C and O. In absence of detailed ab initio calculations, the number of peaks chosen to fit each of the elemental regions was the minimum required to obtain random residuals (thin lines at the bottom of the panels in Figures 2 and 3). For the C and O fits in Figure 3, the peak widths for each element were constrained to the same values. The resulting range of fwhm values for the four major elements in DNA is from ≈1.3 eV for C 1s to ≈1.7 eV for O 1s, values typical for polymer-like materials. A shift to higher BE with increasing DNA coverage is apparent in the N 1s spectra in Figure 2. The shift monotonically increases for the first three samples, saturating at about 0.5 eV for the thickest films in this series (N 1s data in Table 1). Such shifts are common in organic multilayers on metal surfaces and are typically attributed to extra-atomic relaxation and charging effects.[34] The shift is less obvious in the P 2p series in Figure 2, primarily because of the lower signal-to-noise ratio for the first three samples and the intrinsic structure of the 2p doublet. For the C 1s and O 1s regions, the shifts are similar to those for N 1s (not shown).

The principal N 1s core-level peak in Figure 2 has a BE between 400.5 and 401.0 eV, consistent with published results for thymine multilayers (401.1−402.1 eV[27] and 400.4 eV[29]) and powder (400.9 eV[28]). Because very similar chemical shifts are expected for both N atoms in each thymine ring (Figure 1),[35−37] we fit the series shown in Figure 2 using a single main N 1s peak. Two lower BE N 1s components, shifted by approximately −1.8 and −3.1 eV, are observed in Figure 2. A shift to lower BE of this magnitude in organic multilayers has been attributed to

(27) Barber, M.; Clark, D. T. *Chem. Commun.* **1970**, 24−25.
(28) Peeling, J.; Hruska, F. E.; McIntyre, N. S. *Can. J. Chem.* **1978**, *56*, 1555−1561.
(29) Roelfs, B.; Bunge, E.; Schroter, C.; Solomun, T.; Meyer, H.; Nichols, R. J.; Baumgartel, H. *J. Phys. Chem. B* **1997**, *101*, 754−765.
(30) Zhao, Y. D.; Pang, D. W.; Hu, S.; Wang, Z. L.; Cheng, J. K.; Qi, Y. P.; Dai, H. P.; Mao, B. W.; Tian, Z. Q.; Luo, J.; Lin, Z. H. *Anal. Chim. Acta* **1999**, *388*, 93−101.
(31) Wang, J.; Rivas, G.; Jiang, M. A.; Zhang, X. J. *Langmuir* **1999**, *15*, 6541−6545.
(32) Leavitt, A. J.; Wenzler, L. A.; Williams, J. M.; Beebe, T. P. *J. Phys. Chem.* **1994**, *98*, 8742−8746.
(33) Rabkeclemmer, C. E.; Leavitt, A. J.; Beebe, T. P. *Langmuir* **1994**, *10*, 1796−1800.
(34) Sexton, B. A.; Hughes, A. E. *Surf. Sci.* **1984**, *140*, 227−248.
(35) Mely, B.; Pullman, A. *Theor. Chim. Acta* **1969**, *13*, 278−287.
(36) Snyder, L. C.; Shulman, R. G.; Neumann, D. B. *J. Chem. Phys.* **1970**, *53*, 256−267.
(37) Rein, R.; Nir, S.; Hartman, A. *Isr. J. Chem.* **1972**, *10*, 93−100.

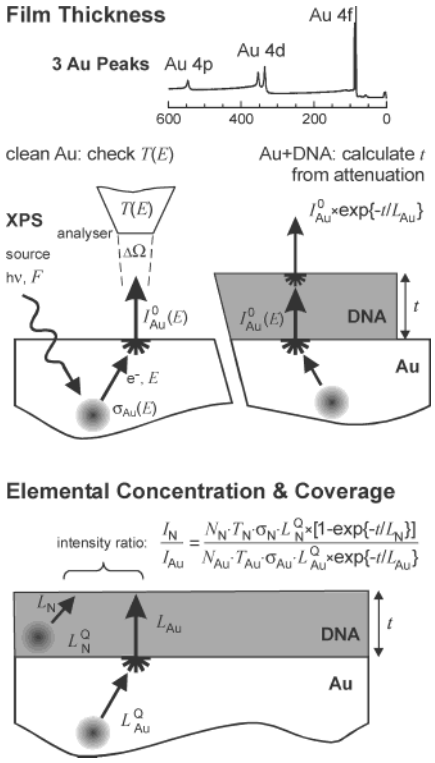

Figure 4. Schematic outline of the analysis procedure. (Top) The measured XPS intensities of three Au peaks at different BEs are compared for spectra from clean Au and Au + DNA samples. Comparison of the intensity attenuation of Au peaks provides a measurement of the film thickness and film uniformity. The peak intensities for clean Au are also used for checking the transmission function $T(E)$ calibration. (Bottom) The DNA film thickness determined in the first step and the calculated values of needed EALs (L's) allow us to calculate the nitrogen atomic concentration in the film N_N relative to N_{Au} from the experimental intensity ratio I_N/I_{Au}.

a strong interaction with the substrate, that is, chemisorption. In fact, the peak shifted by 1.8 eV is consistent with the 1.5 ± 0.2 eV shift reported for thymine chemisorbed on Au(111) in an upright position,[29] and the 3.1 eV shift is comparable to the shift reported for chemisorption of acetonitrile on Pt(111) in a flat geometry.[34] The chemisorbed components are most prominent for the lowest coverage, and both their relative and absolute intensities decrease with increasing coverage. The change in the molecular configuration with increasing coverage suggested by this behavior is considered in detail in a separate paper;[8] for the following discussion, it is only important to note the distinction between the chemisorbed and nonchemisorbed thymine bases.

XPS Data Analysis

The three principal parts of the analysis procedure are discussed in this section (Figure 4). The procedure is based on the standard overlayer XPS formalism. First, the *film thickness* is determined from the attenuation of XPS signals from the gold substrate. An XPS spectrum from a freshly sputtered gold film is used as an absolute intensity reference, and the signal attenuations for the Au 4f, 4d, and 4p peaks are calculated to achieve a consistent result. Second, the obtained film thickness is used to correct measured XPS peak ratios for attenuation within the film and to calculate *elemental concentrations*. The effective attenuation length[38,39] (EAL) for electrons in the film is calculated in both cases using the NIST Standard Reference Database 82 (SRD-82) software.[38−40] Third, relative and absolute *elemental coverage* values are then calculated based on the film thickness and elemental concentrations determined in the first two steps. The choice of model parameters, their uncertainties, and several additional cross-checks are discussed separately in Validation section.

A number of different EALs had to be calculated for this work; for example, note several different L's in Figure 4. To avoid confusion in definitions and terminology, Table 2 lists the notation adopted for EALs in this paper and respective terms used to describe them in a recent review of EAL terminology and definitions[39] and the output of NIST SRD-82 software.[40] The updated EAL definition explicitly defines EAL as a parameter that can be introduced in place of the inelastic mean free path λ (IMFP) into expressions derived from the standard XPS formalism "for a given quantitative application".[39] Thus we need two different types of EALs: "average practical EAL" (PEAL) to be used in expressions with exponential signal attenuation by overlayers and "EAL for quantitative analysis" (QEAL) in intensity prefactors (i.e., expressions related to signal intensity from semi-infinite substrates). While some of the relevant properties of these particular EALs will be noted in the following discussion, full definitions, detailed descriptions, and the appropriate use of these quantities are presented in the above-mentioned comprehensive review.[39]

DNA Film Thickness. The models used for quantitative XPS analysis require specific assumptions and empirical parameters.[41] Unfortunately, the actual structure of ssDNA films on gold under ultrahigh vacuum (UHV) conditions is not known. The model requiring the fewest number of free parameters is the standard uniform overlayer model, which we therefore chose to interpret our data. In this formalism, the observed intensity of the gold substrate signal, I_{Au}, is given by the intensity from a clean gold substrate, I^0_{Au}, attenuated by the DNA film of thickness t as

$$I_{Au} = I^0_{Au} \exp\left[-\frac{t}{L_{Au}}\right] \qquad (1)$$

To obtain the film thickness from this equation, the PEAL for electrons from Au in the DNA film, L_{Au}, needs to be calculated for each of the measured Au substrate peaks (4f, 4d, and 4p). The calculations are performed using NIST SRD-82 software[40] based on the kinetic energy (KE) of the electrons and the following overlayer parameters: stoichiometry coefficients, number of valence electrons per molecule, band-gap energy (E_g), and density (ρ_{DNA}). The choice of values for the latter two parameters is not a simple matter for a DNA film and is discussed in detail in DNA Film Parameters section. The calculated $(dT)_{25}$−SH ssDNA film thickness values, listed in Table 3, are based on the data for the three Au peaks from the 1−1200 min immobilization series. The PEALs for a film of 5 nm thickness, as listed in Table 3, were used to determine the film thickness in all cases. Note that the PEALs calculated for a 2 nm thick film differ from those for a 5 nm film by not more than 0.4% (Table 3), so this simplification does not introduce an appreciable systematic error into the analysis.

(38) Powell, C. J.; Jablonski, A. *Surf. Interface Anal.* **2002**, *33*, 211−229.
(39) Jablonski, A.; Powell, C. J. *Surf. Sci. Rep.* **2002**, *47*, 35−91.
(40) Powell, C. J.; Jablonski, A. *NIST Electron Effective-Attenuation-Length Database, Version 1.0 (SRD-82)*; U.S. Department of Commerce, National Institute of Standards and Technology: Gaithersburg, MD, 2001.
(41) Fulghum, J. E.; Linton, R. W. *Surf. Interface Anal.* **1988**, *13*, 186−192.

Table 2. EAL Notation and Terminology

variable	descriptive summary	formal description[a]	SRD-82 description & parameters
L_{Au}	PEAL for electrons from Au in DNA film	"average practical EAL" for electrons from Au in DNA *overlayer*[b]	"Average EAL (Lave)" in "Practical and average EALs" output window. Calculated using kinetic energy and β for Au electrons; DNA film parameters.
L_X	PEAL for electrons from DNA elements (X = N, P, C, O) in DNA film	"average practical EAL" for electrons from DNA in DNA *overlayer*[b]	"Average EAL (Lave)" in "Practical and average EALs" output window. Calculated using kinetic energy and β for X electrons; DNA film parameters.
L^Q_{Au}	QEAL for electrons from Au in Au film	"EAL for quantitative analysis" for *semi-infinite* Au substrate[c]	"EAL for quantitative analysis" in "Practical and average EALs" output window ("Related parameters" section). Calculated using kinetic energy and β for Au electrons; "Recommended IMFP values" for elemental Au from the SRD-82 database.
L^Q_X	QEAL for electrons from DNA elements (X = N, P, C, O) in DNA film	"EAL for quantitative analysis" for *infinitely thick* DNA overlayer[c]	"EAL for quantitative analysis" in "Practical and average EALs" output window ("Related parameters" section). Calculated using kinetic energy and β for X electrons; DNA film parameters.

[a] Formal terminology follows that of a recent EAL review (section 9.1 for PEAL, section 8.3 for QEAL) (ref 39). [b] "Average practical EAL" is explicitly defined as a parameter to be used for *overlayers* with approximately exponential attenuation. Because DNA is the only type of overlayer considered in this paper, in all cases PEALs refer to attenuation by the DNA film of electrons from the specified element.[c] "EAL for quantitative analysis" is defined and calculated based on an expression for XPS intensity from semi-infinite substrates; i.e., the same type of expression that serves as a prefactor in front of the exponential attenuation terms. By definition, QEALs refer to electrons originating in a material and attenuated within the material itself, such as Au electrons in Au or N, P, C, and O electrons in a DNA film.

Table 3. Attenuation of Gold Substrate Peak Intensities and DNA Film Thickness *t*

immobilization time (min)	Au $4f_{7/2}$ L_{Au4f}=3.858 nm[a]		Au $4d_{5/2}$ L_{Au4d}=3.274 nm[a]		Au $4p_{3/2}$ L_{Au4p}=2.764 nm[a]	
	I_{Au}/I^0_{Au}	t (nm)[b]	I_{Au}/I^0_{Au}	t (nm)[b]	I_{Au}/I^0_{Au}	t (nm)[b]
1	0.568	**2.18**	0.518	**2.15**	0.480	**2.03**
5	0.525	**2.49**	0.467	**2.49**	0.432	**2.32**
30	0.449	**3.09**	0.387	**3.11**	0.305	**3.28**
120	0.360	**3.94**	0.286	**4.10**	0.201	**4.43**
1200	0.254	**5.29**	0.203	**5.22**	0.125	**5.75**

[a] PEALs (L_{Au}) for electrons from the Au substrate in the DNA film were calculated using NIST SRD-82 software (ref 40) with the following parameters: experimental kinetic energy for Au photoelectrons; asymmetry parameters β for electrons Au $4f_{7/2}$ (β = 1.04), $4d_{5/2}$ (β = 1.22) (ref 40), and Au $4p_{3/2}$ (β = 1.63) (ref 42); ideal stoichiometry of dT nucleotides (Figure 1); band-gap energy E_g = 4.8 eV; film density ρ_{DNA} = 0.893 g/cm^3. PEAL or "average practical EAL" values (Table 2) calculated for a film of 5 nm thickness are listed in each case. For comparison, PEALs calculated for a 2 nm film are L_{Au4f} = 3.869 nm, L_{Au4d} = 3.283 nm, and L_{Au4p} = 2.775 nm. [b] DNA film thickness t calculated from experimental Au signal attenuation (eq 1).

The peak intensity ratios I_{Au}/I^0_{Au} listed in Table 3 were determined from fits to experimental Au $4f_{7/2}$, $4d_{5/2}$, and $4p_{3/2}$ spectra. The reference clean Au spectra (I^0_{Au}) were acquired from a gold film immediately after Ar ion sputtering. The estimates of the DNA film thickness listed in Table 3 were obtained by substitution of experimental intensity ratios into eq 1. Note that there is a variation of several hundred electronvolts in KE of electrons between the three Au peaks; thus, the agreement between these semi-independent estimates is a good indication that the simple uniform overlayer model is suitable for this system. Only for the two thickest films, the Au 4p thickness appears ≈10% larger than the Au 4f and 4d estimates. Note, however, that 4p has the lowest KE of the three Au peaks and thus experiences the strongest attenuation. Strong attenuation affects the thickness estimate in two ways: the combination of a low peak intensity and high inelastic background means that the fitting procedure is subject to a greater uncertainty, and the assumption of approximately exponential attenuation may not be valid.[39] Conversely, the most reliable estimate is that from the Au $4f_{7/2}$ peak because it has the highest intensity, the weakest attenuation, and the smallest uncertainty due to the inelastic background fitting. Therefore, we use the film thickness values shown in Table 3 from the Au $4f_{7/2}$ peak attenuation in the subsequent analysis.

Elemental Concentrations and Stoichiometry. Once the film thickness is known, elemental concentrations can be determined. In the simple overlayer model, the intensity of the XPS signal, I_X, originating from atoms of element X in the film is given by

$$I_X = I^\infty_X\left[1 - \exp\left(-\frac{t}{L_X}\right)\right] \qquad (2)$$

where I^∞_X is the intensity from bulk material, and the term in the square brackets accounts for the finite thickness of the film and for attenuation of the signal with a PEAL of L_X.

The remaining factors in eqs 1 and 2 that must be considered to determine the elemental concentrations are the prefactors I^0_{Au} and I^∞_X (the XPS signal intensities from bulk gold and DNA samples, respectively). According to standard XPS formalism,[39,41] a prefactor can be expressed as

$$I = \{FA\ \Delta\Omega\}T\ \ \sigma\ W(\beta,\psi)\ \lambda N \qquad (3)$$

where F is the incident X-ray flux, A is the analyzed sample area, $\Delta\Omega$ is the acceptance solid angle of the analyzer, T is the analyzer transmission function, σ is the total photoelectric cross section, $W(\beta,\psi)$ is the angular distribution term, λ is the IMFP, and N is the atomic density for the chemical element observed (what we want to determine).

The first three factors, $\{FA\ \Delta\Omega\}$, are grouped together because they cancel out when experimental intensity *ratios* are measured. The analyzer transmission function (T) is calibrated and provided by the instrument manufacturer; we also checked this calibration by comparing normalized peak intensities for a clean Au substrate, as explained in Instrument-Related Factors section. We used standard,

Table 4. EAL Values Calculated[a] for Au and the Four Major Elements in DNA for Use in Elemental Analysis

peak	PEAL in DNA film L (nm)	QEAL L^Q (nm)[b]
C 1s	3.391	3.529
O 1s	2.798	2.938
N 1s	3.116	3.255
P $2p_{3/2}$	3.754	3.860
Au $4f_{7/2}$	3.858	1.745[b]

[a] Specified EALs were calculated using SRD-82 software (ref 40) with parameters as given for Table 3 and two additional asymmetry parameters, β, for photoelectrons (ref 40): $\beta = 2$ for 1s peaks and $\beta = 1.1$ for P $2p_{3/2}$. [b] Values of QEAL (refs 39 and 40), L^Q, are calculated for the material in which the photoelectrons originate; i.e., the DNA film for the C, O, N, and P and the gold substrate for the Au. The L^Q_{Au} value for Au was calculated based on the recommended IMFP values from the SRD-82 database (ref 40).

tabulated Scofield coefficients[43] for the total photoelectric cross section, which is justified for our experimental geometry (normal emission and the 58° X-ray angle of incidence). Following the suggestion of ref 39, we can use QEAL values (L^Q) calculated by the SRD-82 software[40] in place of the IMFP (λ). This substitution accounts for the effect of elastic collisions on the photoelectron intensities and their angular distributions. Note that L^Q is explicitly defined such that the modified angular distribution factor cancels out in intensity ratios.[39]

Finally, we determine the atomic density N_X for each of the four elements in the DNA film (X = C, O, N, and P). From each ratio of the measured intensities from the film I_X and the gold substrate I_{Au}, we can determine the ratio of the selected elemental atomic density to that of gold (N_X/N_{Au}) combining eqs 1−3 as

$$\frac{N_X}{N_{Au}} = \frac{I_X}{I_{Au}} \frac{T_{Au}\sigma_{Au}L^Q_{Au}}{T_X\sigma_X L^Q_X} \frac{\exp[-t/L_{Au}]}{1 - \exp[-t/L_X]} \qquad (4)$$

As we discussed above, t can be taken from Table 3, and L^Q_X, L^Q_{Au}, L_X, and L_{Au} are the QEALs and PEALs[39] calculated by the SRD-82 program,[40] respectively (as tabulated in Table 4). If we assume the accepted gold density of 19.28 g/cm^3, the atomic density of gold is $N_{Au} = 5.892 \times 10^{22}$ atoms/cm^3. The absolute atomic density of the element X in the film can be determined from eq 4.

To determine the DNA coverage, we use nitrogen as the reference signal because it is specific to DNA molecules, not subject to contamination from the environment, and has a clean spectral signature for $(dT)_{25}$−SH ssDNA films[8] (Figure 2). The ratios of other elemental concentrations to nitrogen can then be compared to stoichiometric ratios for the five films in the series (Table 5). Note that these ratios were calculated using eq 4 and thus include the effect of the XPS signal attenuation in the film. The P/N ratio is constant within the experimental ±10% data scatter, indicating that there is no preferential damage or desorption of the phosphate backbone compared to the N-substituted thymine rings. Both the C/N and O/N ratios decrease to almost stoichiometric values with increasing DNA film thickness, indicating that the ssDNA films are not hydrated under the UHV conditions [the O/N ratio for the thickest film indicates less than one extra oxygen atom (water molecule) per nucleotide] and that there is little nonspecific coadsorption of adventitious hydrocarbons on the thick DNA films. The apparent DNA film density,

Table 5. Calculated Elemental Concentrations and Stoichiometry of $(dT)_{25}$ Films

immobilization time (min)	P/N ratio[a] (ideal 0.5)	C/N ratio[a] (ideal 5)	O/N ratio[a] (ideal 3.5)	% expected N concn (ideal 100)[b]	ρ_{DNA}[c] g/cm^3
1	0.60	8.3	4.3	71	0.59
5	0.54	6.3	4.3	82	0.84
30	0.56	5.7	4.0	89	0.94
120	0.55	6.2	4.0	85	0.94
1200	0.64	5.8	3.8	89	0.89

[a] Calculated elemental ratios take into account the photoelectron attenuation in the film (eq 4). [b] Observed atomic fraction of N in the film as a percentage of the 1/10 expected for a stoichiometric dT film. [c] The density of the DNA film, ρ_{DNA}, calculated from the nitrogen atomic concentration (N_N) assuming the ideal dT stoichiometry.

Table 6. Nitrogen Atomic Concentration N_N and Absolute Coverage of $(dT)_{25}$ DNA n_{T25}

immobilization time (min)	DNA film thickness t (nm)	atomic density of N relative to Au, N_N/N_{Au}	relative N coverage θ_N/N_{Au}	DNA coverage n_{T25} ($\times 10^{13}$ DNA/cm^2)
1	2.2	0.0390	0.086	1.0
5	2.5	0.0557	0.139	1.6
30	3.1	0.0623	0.193	2.3
120	3.9	0.0624	0.243	2.9
1200	5.3	0.0591	0.313	3.7

ρ_{DNA}, can be calculated from the N_N/N_{Au} ratio and mass fraction of N in DNA. Assuming the expected stoichiometry for oligo(dT) ssDNA, $\rho_{DNA} = N_N/N_{Au} \times 15.05$ g/cm^3.[44] We attribute the apparently low DNA film density for short immobilization times (Table 5) to the relatively large amount of coadsorbed hydrocarbons, which remain unaccounted for in the stoichiometric formula for ρ_{DNA}.

DNA Coverage. The number of nitrogen atoms per unit area of the film, θ_N, is obtained by multiplying the atomic density N_N by the film thickness t,

$$\theta_N = N_N t \qquad (5)$$

Because N_N is not measured directly, but rather as a N_N/N_{Au} ratio, a more practical quantity to consider is the relative N coverage θ_N/N_{Au}, which is then simply a product of two measured quantities (Table 6). Note that when defined this way, the relative nitrogen coverage is proportional to the absolute coverage and therefore can be used to quantitatively compare coverage (based on a specific element) for samples with essentially arbitrary film stoichiometry. If the proper film stoichiometry is known, the absolute coverage can be calculated from θ_N/N_{Au} as well; for example, for $(dT)_{25}$−SH,[45]

$$n_{T25} = \theta_N/N_{Au} \times 11.78 \times 10^{13} \text{ molecules/cm}^2 \qquad (6)$$

A very important property of the relative N coverage θ_N calculated from eq 5 is revealed if eqs 4 and 5 are rewritten as

$$\frac{\theta_N}{N_{Au}} = \left\{\frac{I_N}{I_{Au}} \frac{T_{Au}\sigma_{Au}L^Q_{Au}}{T_N\sigma_N}\right\} \frac{t}{L^Q_N} \frac{\exp[-t/L_{Au}]}{1 - \exp[-t/L_N]} \qquad (7)$$

Here the prefactor in curly braces includes only parameters known or directly measured and independent of the EAL

(42) Yeh, J. J.; Lindau, I. *Atom. Data Nucl. Data Tables* **1985**, *32*, 1−155.

(43) Scofield, J. H. *J. Electron Spectrosc. Relat. Phenom.* **1976**, *8*, 129−137.

(44) For gold, density $\rho_{Au} = N_{Au}M_{Au}$, where $M_{Au} = 197$ is the atomic mass of gold. For DNA, $\rho_{DNA} = N_N M_{DNA}/[\#N]$, where $M_{DNA} = 7691$ is the molecular mass of $(dT)_{25}$−SH and $[\#N] = 50$ is the number of N atoms in one $(dT)_{25}$−SH molecule. Combining the above expressions, we obtain the numerical conversion factor between ρ_{DNA} in g/cm^3 and N_N/N_{Au} to be 19.28 × (7691/50)/197 = 15.05.

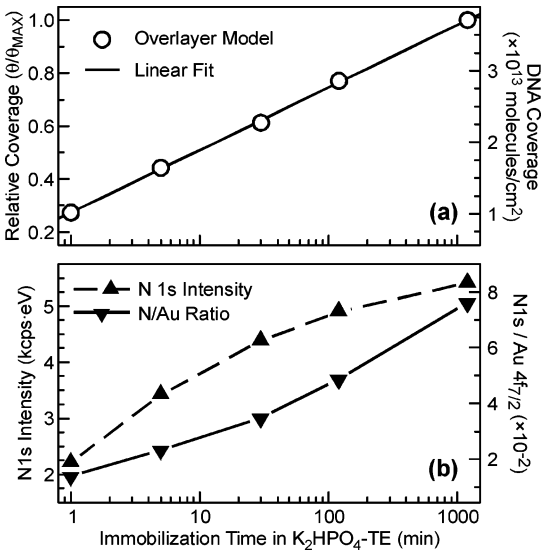

Figure 5. Three quantification methods for $(dT)_{25}-SH$ ssDNA coverage as a function of immobilization time in 1 M K_2HPO_4−TE buffer. (a) Open circles are coverage values calculated based on the total N 1s XPS signal (Figure 2). The relative coverage (left axis) is normalized to the maximum value. The absolute coverage (right axis) is calculated using the overlayer−substrate model. The solid line is a linear-to-log-time fit to the data. (b) Relative "coverage" analysis for the two simpler commonly used quantification methods, the raw N 1s XPS intensity (up triangles, left axis) and the ratio of the N 1s and Au $4f_{7/2}$ intensities (down triangles, right axis). Lines are provided to guide the eye.

calculations for DNA films. Note that the film thickness t and the calculated EALs (L) only enter eq 7 as *t/L ratios*. As we will discuss below in Invariant EAL Ratios section, these ratios are very insensitive to uncertainties in the DNA film parameters used to calculate the EALs. Therefore, the property we are most interested in, the absolute DNA coverage, is actually the one we can determine with the least uncertainty.

The evolution of the DNA coverage as a function of the immobilization time is shown in Figure 5a. The coverage (from Table 6) has been calculated based on the total intensity of the N 1s signal for this immobilization series (Figure 2) using eqs 4 and 5 with the film thickness data in Table 3. The relative coverages (left axis in Figure 5a) are normalized to the observed maximum coverage after 1200 min of immobilization. Absolute coverage values (right axis in Figure 5a) were calculated from eq 6. The absolute coverage after immobilizing $(dT)_{25}-SH$ for 1200 min is 3.7×10^{13} molecules/cm^2, in good agreement with the value of 3.0×10^{13} molecules/cm^2 determined by radiolabeling for a thiol-modified 24-base-long ssDNA immobilized under the same conditions.[10]

Note the apparent linear-in-log-time kinetics in Figure 5a, which is highly unusual for an adsorption process.[8] Langmuir-like behavior, typically assumed for adsorption of thiol-functionalized molecules on gold, would produce a nonlinear curve in these coordinates (e.g., Figure 11 in ref 23). Some model calculations for polyelectrolyte adsorption at high salt concentrations predict a kinetics curve with an asymptotically linear immobilization time dependence, where the molecular reorganization at the surface becomes the rate-limiting step.[46] As discussed elsewhere,[8] there is other evidence that such a reorganization indeed happens during the immobilization of $(dT)_{25}-SH$ ssDNA on gold.

Validation

Instrument-Related Factors. The expression for the XPS intensity given by eq 3 contains two instrument-dependent factors:[41] the $\{FA\,\Delta\Omega\}$ product (determined by the instrument geometry, configuration, settings, and stability) and the analyzer transmission function, T (determined by the instrument design, settings, and stability). The first group of parameters is assumed to cancel out when intensity ratios are considered in our analysis (eq 4). We used the analyzer transmission function values provided by the manufacturer and checked them using a clean Au spectrum, as explained at the end of this section. We estimate the contributions to the overall measurement uncertainty due to these instrument-related factors to be 5−10%, as explained below.

The elemental analysis (eq 4) is based on *relative intensities*, that is, on intensities for all elements acquired without changing the position or orientation of the sample, so that the geometric factors A and $\Delta\Omega$ do not contribute. The acquisition time for the N and P spectra was typically 30−50 times longer than that for the Au 4f region, and thus fluctuations in the X-ray flux F introduce an uncertainty. In our standard procedure, two sets of spectra for the Au 4f region were acquired, one immediately before and the other after completing the rest of the elemental regions. The typical difference in intensity between these two spectra was <2% and never more than 5% (both positive and negative changes have been observed). Because the calculated value of the coverage depends linearly on the ratio of the elemental intensity for N to Au intensity (eqs 4 and 5), the above flux fluctuations contribute linearly to the overall uncertainty.

The thickness of DNA films was determined from ratios of *absolute Au intensities* (eq 1). When the intensities of Au peaks were compared for the DNA-covered and freshly cleaned gold samples, variation of all three parameters in the $\{FA\,\Delta\Omega\}$ group contributed to uncertainty. For practical reasons, the clean reference samples were typically measured at the end of a run (in previous calibration studies, such reference samples were periodically measured throughout several hours). The relevant timescale for the X-ray flux (F) variability was then longer for the thickness measurements, resulting in an increased uncertainty of ≈5%. The maximum count rate was used to define the measurement position for each sample. The variability in geometric factors A and $\Delta\Omega$ for this positioning procedure has been previously considered in systematic studies[47−49] and is estimated to be about 10%. Our operational mode of the XPS spectrometer included use of a magnetic lens, which tends to reduce the variability in the effective collection solid angle ($\Delta\Omega$) caused by small changes in sample position and orientation. In addition, the positioning uncertainty is decreased since we use an X-ray monochromator. Because both the incident X-ray beam and the photoelectron trajectories are focused, the optimal measurement position is well-defined.[49] The DNA

(45) To convert between the atomic density of gold $N_{Au} = 5.892 \times 10^{22}$ atoms/cm^3 and the $(dT)_{25}-SH$ surface density n_{T25}, the numerical factor is given by $(5.892 \times 10^{22}) \times 10^{-7}/50 = 11.78 \times 10^{13}$, where the factor 10^{-7} accounts for film thickness expressed in nanometers rather than centimeters, and 50 is the number of nitrogen atoms per $(dT)_{25}-SH$ molecule.

(46) Cohen Stuart, M. A.; Hoogendam, C. W.; de Keizer, A. *J. Phys.: Condens. Matter* **1997**, *9*, 7767−7783.
(47) Powell, C. J.; Seah, M. P. *J. Vac. Sci. Technol., A* **1990**, *8*, 735−763.
(48) Cumpson, P. J. *J. Electron Spectrosc. Relat. Phenom.* **1995**, *73*, 25−52.
(49) Seah, M. P.; Gilmore, I. S.; Spencer, S. J. *Surf. Interface Anal.* **1998**, *26*, 617−641.

layer thickness (t) depends on these ratios of absolute Au intensities logarithmically (eq 1). Note that the resulting uncertainty in t from these effects is typically less than the scatter in the values of t obtained from the different Au peaks and from measurements in multiple spots on a sample.

Another source of uncertainty in the thickness measurements is the rather large effective acceptance cone of the magnetic lens. The acceptance angle is ±4° along the energy dispersive direction and ±30° along the nondispersive direction. The collected signal then does not strictly correspond to normal emission. Explicitly accounting for the resulting distribution of emission angles would require sophisticated modeling because a cosine of each off-normal angle must be introduced in eqs 1, 2, and 4. However, even for the larger of the two acceptance angles, the average value of the cosine factor is ≈0.95; thus, including the angular distributions would not change the calculated thickness values by more than ≈5%. The additional systematic uncertainty in t related to the acceptance cone then does not change our overall estimate discussed above.

To test the values of the *analyzer transmission function* (T) provided by the manufacturer, the relative intensities of Au 4f, 4d, and 4p peaks were compared for a freshly sputter-cleaned gold substrate. Like the measurements of relative intensities described above for the other elements, the intensity of each of the Au peaks is given by eq 3, and the geometric factors cancel out when intensity ratios are considered. When the appropriate values of the transmission function, Scofield sensitivity factors,[43] and calculated QEALs are used to normalize the Au peak intensity ratios, they are reduced to ratios of the atomic density of gold, ideally ≡1. The experimental intensities of the three peaks normalized in this manner are within 6% of unity, a satisfactory result given the uncertainty in the Au 4d and 4p peak intensities caused by the inelastic background subtraction during fitting. QEAL values were used in place of IMFP in eq 3, as suggested in ref 39, and they were determined from the "recommended IMFP values"[40] for Au. The Au 4f, 4d, and 4p peaks span the energy range that contains all the elemental peaks for major elements in DNA, so the above normalization procedure is an effective test of the analyzer transmission function factors used in our analysis.

DNA Film Parameters. The SRD-82 software requires a number of parameters to adequately specify the film properties for the EAL calculations.[40] As suggested by the software developers, we chose the predictive TPP-2M formula[50] to determine the IMFPs for the organic films in our study. The following parameters are included in the TPP-2M formula implemented in the SRD-82 software:[40,50] film elemental composition, number of valence electrons per molecule, band-gap energy, and film density. Below we discuss the values for all these parameters that we found appropriate for the DNA films in our study. The most important conclusion of the following discussion is that, for any self-consistent set of parameters, small differences between the assumed and "true" values for a particular film have little effect on the calculated values of the coverage (eqs 4, 5, and 7). In terms of the measurement uncertainty, this means that random contributions such as changes in film stoichiometry or inaccurate values of the band-gap do not contribute appreciably to the uncertainty of the calculated coverage. The main contribution to the uncertainty from the DNA film parameters arises from a systematic uncertainty of the EAL calculations, which has been estimated to be about 15−20% by the authors of the TPP-2M formula.[40,50] This estimate includes two separate contributions: the uncertainty of IMFPs calculated using the TPP-2M formula[40,50] and the validity of the algorithm used for EAL calculations.[51]

Table 7. Self-Consistent Values of the DNA Film Density (ρ_{DNA}) and Thickness (t_{1200}) for the 1200 min Sample Calculated for a Range of Assumed Band-Gap Energies (E_g)

E_g (eV)	ρ_{DNA} (g/cm^3)	t_{1200} (nm)	E_g (eV)	ρ_{DNA} (g/cm^3)	t_{1200} (nm)
4.0	0.925	5.12	6.0	0.845	5.62
4.6	0.900	5.24	8.0	0.720	6.55
4.8	**0.893**	**5.29**	10.0	0.570	8.34
5.0	0.885	5.34			

The DNA film composition was entered into the SRD-82 software assuming the ideal stoichiometry of the dT nucleotide (Figure 1). The data in Table 5 suggest that this assumption is approximately correct for the thicker films in the series. Because of the similarity in atomic number and number of electrons between the dominant elements in these organic films, even if the relatively C- and O-rich stoichiometry we observe is input in the software, the resulting EAL values change at most by a few percent. We chose to keep as many parameters as possible fixed throughout our data analysis, and we therefore assumed the ideal stoichiometry values in all cases. *The number of valence electrons per molecule* is also determined based on the assumed ideal stoichiometry, following the formula suggested for the SRD-82 software.[40]

DNA was one of the 14 organic compounds in the data set used to derive the TPP-2M predictive formula for IMFPs.[50] The values of the *band-gap energy* (E_g) and *film density* (ρ_{DNA}) used for DNA in this original derivation were obtained from an early UV-transmission study.[52] However, in that UV study a thick, dried, self-supported film composed of long fragments of double-stranded DNA (dsDNA) was measured,[52] so the E_g and ρ_{DNA} values obtained may not be applicable to the surface-immobilized films of short (25 bases) ssDNA pieces in our experiments.

Fortunately, E_g and ρ_{DNA} are not independent parameters in our analysis procedure. For a given value of E_g, an initial estimate of ρ_{DNA} can be used to carry out the analysis and determine a film density from the data and eq 4. We then use this new value of ρ_{DNA} to repeat the analysis until the value of ρ_{DNA} converges self-consistently. Several such *self-consistent values of* ρ_{DNA} are listed in Table 7.

The band-gap energy remains as the only relevant property of the ssDNA film that is not well-defined. Of course, one typically associates molecular orbitals, not band structure, with molecular species such as DNA. For solid state materials, the band-gap is typically determined from electrical transport or optical absorption properties. Although there has been considerable interest in the transport properties of DNA,[53−55] to our knowledge there have been no transport measurements or calculations appropriate for use in understanding inelastic electron scattering in DNA films.

For a material with a band-gap, both the electron inelastic scattering probability and the UV absorption

(50) Tanuma, S.; Powell, C. J.; Penn, D. R. *Surf. Interface Anal.* **1994**, *21*, 165−176.

(51) Jablonski, A.; Powell, C. J. *Surf. Sci.* **2002**, *520*, 78−96.

(52) Inagaki, T.; Hamm, R. N.; Arakawa, E. T.; Painter, L. R. *J. Chem. Phys.* **1974**, *61*, 4246−4250.

(53) Iguchi, K. *J. Phys. Soc. Jpn.* **2001**, *70*, 593−597.

(54) Ye, Y. J.; Jiang, Y. *Int. J. Quantum Chem.* **2000**, *78*, 112−130.

(55) Ye, Y. J.; Chen, R. S.; Martinez, A.; Otto, P.; Ladik, J. *Physica B* **2000**, *279*, 246−252.

Table 8. Invariant Ratios of the Calculated PEALs and QEALs to Film Thickness (t_{1200}) for Two Extreme Values of the Band-Gap Energy (E_g)

	$E_g = 10$ eV, $\rho_{DNA} = 0.570$ g/cm^3		$E_g = 4$ eV, $\rho_{DNA} = 0.925$ g/cm^3	
peak	PEAL in DNA film L (nm)	L/t_{1200}	L/t_{1200}	PEAL in DNA film L (nm)
C 1s	5.340	0.643	0.644	3.283
O 1s	4.400	0.530	0.531	2.709
N 1s	4.903	0.591	0.592	3.017
P $2p_{3/2}$	5.916	0.713	0.713	3.634
Au $4f_{7/2}$	6.085	0.733	0.733	3.737
	$E_g = 10$ eV, $\rho_{DNA} = 0.570$ g/cm^3		$E_g = 4$ eV, $\rho_{DNA} = 0.925$ g/cm^3	
peak	QEAL in DNA film L^Q (nm)	L^Q/t_{1200}	L^Q/t_{1200}	QEAL in DNA film L^Q (nm)
C 1s	5.559	0.670	0.670	3.417
O 1s	4.621	0.557	0.558	2.845
N 1s	5.124	0.617	0.618	3.152
P $2p_{3/2}$	6.086	0.733	0.733	3.738

have essentially the same threshold energy, because both are proportional to the imaginary part of the dielectric constant. Thus, we consider the *threshold* in UV absorption observed for dsDNA and ssDNA in solution and on surfaces to be the most appropriate experimental estimate of the band-gap. Typically, DNA in solution is characterized by measuring the UV absorption *peak* (usually at 260 nm).[56] The position of the absorption peak varies slightly between the nucleotides in solution[56] (dA, 250 nm; dC, 271 nm; dG, 250 nm; dT, 267 nm) and homo-oligonucleotides on surfaces[57] [$(dA)_{20}$, 272 nm; $(dC)_{20}$, 255 nm; $(dG)_{20}$, 255 nm; $(dT)_{20}$, 262 nm]. We use $E_g = 4.8$ eV, which corresponds to the average value for the UV absorption peak (258 nm). Note that the UV absorption threshold is typically about 0.5 eV below the peak, so the peak energy is an upper limit for the actual band-gap. The self-consistent value of the film density using 4.8 eV is 0.893 g/cm^3 (Table 7). Also note that neither the EAL nor the film density change dramatically for values of E_g between 4 and 5 eV (Table 7).

Invariant EAL Ratios. The physical model behind the TPP-2M predictive formula[50] is very robust with respect to the choice of film parameters. As explained above, the only independent parameter in our analysis procedure is the band-gap energy. To illustrate the effect of this parameter, EALs in the DNA film for all five elements analyzed here have been calculated for two extreme values of E_g, 4 and 10 eV (Table 8). The apparent film photoelectron thicknesses calculated based on the two resulting EALs for Au 4f are of course different (Table 7). However, the ratios of EALs to the respective film thicknesses are *essentially identical*, as listed in Table 8. This invariance is to be expected for the Au 4f EALs by construction (eq 1), but for the rest of the peaks it only happens because of the nearly-linear IMFP dependence on the KE (in the energy range of interest) in the model that produced the TPP-2M equation.[50]

The importance of this observation for our analysis is that any value that depends only on the *ratios* of calculated EALs to the respective film thickness (L/t) is essentially independent of the particular *self-consistent* values of E_g and ρ_{DNA} used to describe the film. In other words, any of the E_g and ρ combinations from Table 7 will yield the same DNA coverage. In fact, even values of E_g and ρ_{DNA} that are not self-consistent (e.g., $E_g = 4$ eV and $\rho_{DNA} = 1.3$ g/cm^3 after ref 52) yield similar coverages. Therefore, changes in the film volume density or elemental stoichiometry as large as 50% do not change the quantitative results of interest by more than a few percent, including the *relative concentrations* of the elements and the *DNA coverage*. Furthermore, we can neglect potential variations of the film density and stoichiometry with coverage and analyze all films using parameters determined from the thickest, most bulklike film.

In contrast to the relative elemental concentrations and DNA coverage, the calculated value of the film thickness can depend strongly on the parameters assumed for the DNA film (Table 7). Thus, the values of t listed in Table 3 should be considered approximate, only as reliable as our choice of the empirical model parameters (E_g and ρ_{DNA} in particular). As discussed in the previous section, we made an effort to choose the most appropriate values of E_g and ρ_{DNA}. These values are similar to those from the early UV study,[52] which were subsequently used to derive the TPP-2M equation[50] and a recently proposed alternative method[58] for estimating IMFPs for polymers. As a result, the EAL and film thickness values in Table 3 are consistent with the predictions for DNA from those two methods.[50,58] Note that within the most likely range of the effective band-gap energy values for a DNA film (4−5 eV), the variation of calculated film thickness values is only about 4% (Table 7). To summarize, the values of film parameters and thickness in Tables 3−5 can be treated as a reliable, self-consistent set for use with the XPS analysis presented here; however, their correspondence to the actual properties of ssDNA films under UHV conditions is less certain.

Testing the Simple Exponential Attenuation Assumption. One of the most important factors in our method for quantitative XPS analysis of DNA films is an accurate accounting of the signal attenuation in the DNA film, a factor briefly addressed in DNA Film Thickness section. Here we offer several additional consistency checks along with a comparison with FTIR spectroscopy results to further validate our analysis method.

Two much simpler methods than ours are often used for qualitative evaluation of the film coverage based on XPS data, the overlayer/substrate signal ratio and the absolute overlayer signal intensity. The apparent immobilization kinetics that is inferred from these two methods is shown in Figure 5b. Both of these methods give results that are notably different from the linear-in-log-time dependence produced by the overlayer/substrate model (Figure 5a). Measuring the ratio of the N 1s to the Au $4f_{7/2}$ peak intensities overestimates the coverage for thick films because the Au signal is attenuated more strongly than the N. Conversely, the absolute intensity of the N 1s signal underestimates the coverage for thick films because there is some attenuation of the N signal. The contrast between the results in panels a and b of Figure 5 clearly demonstrates that signal attenuation in the film is significant for photoelectrons from both the substrate and the overlayer and that both effects must be properly included in the analysis.

Ideally, one would like a direct measurement of intensity versus film thickness to determine the functional dependence of the signal attenuation. For example, in alkanethiol self-assembled monolayers (SAMs) an exponential attenuation of the substrate photoelectron signal has been directly observed by varying the number of carbon atoms in the chain to systematically vary the film thickness.[17,59,60]

(56) Sober, H. A., Ed. *CRC Handbook of Biochemistry*: *Selected Data for Molecular Biology*; Chemical Rubber Co.: Cleveland, 1968.

(57) Thomas, C. W.; Saprigin, A. V.; Spector, M. S. Personal communication.

(58) Cumpson, P. J. *Surf. Interface Anal.* **2001**, *31*, 23−34.

(59) Lamont, C. L. A.; Wilkes, J. *Langmuir* **1999**, *15*, 2037−2042.

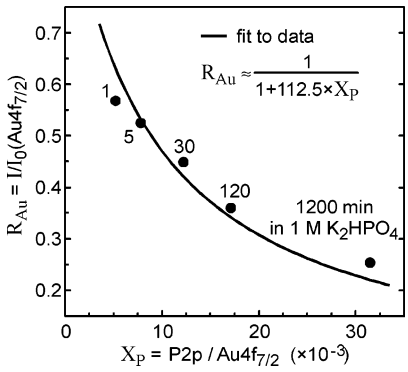

Figure 6. Empirical check of the exponential attenuation model (eq 11). For each sample in the 1 μM $(dT)_{25}$−SH immobilization series, a data point on this plot is defined by two ratios of experimental peak intensities: P 2p/Au 4f $_{7/2}$ (X_P, *x*-axis), and Au 4f $_{7/2}$ with and without the DNA film (R_{Au}, *y*-axis). A fit to the simple functional form of eq 11 is shown, with the best fit achieved with $112.5X_P$, vs $112X_P$ as predicted for eq 11.

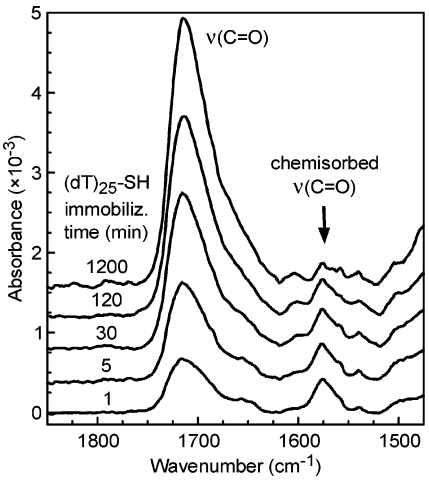

Figure 7. Evolution of FTIR absorption spectra with increasing immobilization time for 1 μM $(dT)_{25}$−SH in 1 M K_2HPO_4−TE buffer. The peak at 1714 cm^{-1} corresponds to carbonyl groups in free thymine rings (and is specific to dT nucleotides). Peaks in the 1550−1600 cm^{-1} region are attributed to chemisorbed thymine.

There is no comparably simple parameter related to film thickness for DNA [e.g., one cannot assume that a $(dT)_{25}$ film is 5 times thicker than one of $(dT)_5$].

The small difference in the KE of P 2p and Au 4f photoelectrons (≈50 eV) suggests one approach to measuring the signal attenuation in our films. For these photoelectrons, eq 4 can be rewritten as

$$\frac{I_P}{I_{Au}} = \frac{T_P}{T_{Au}} \frac{\sigma_P L_P^Q}{\sigma_{Au} L_{Au}^Q} \frac{N_P}{N_{Au}} \frac{1 - \exp[-t/L_P]}{\exp[-t/L_{Au}]} \tag{8}$$

or

$$\frac{I_P}{I_{Au}} \approx \frac{\sigma_P L_P^Q}{\sigma_{Au} L_{Au}^Q} \frac{N_P}{N_{Au}} \frac{1 - \exp\left[-\frac{t}{L}\right]}{\exp\left[-\frac{t}{L}\right]} \tag{9}$$

where we assume $T_P \approx T_{Au} = T$ and $L_P \approx L_{Au} = L$ because of the approximately equal electron energies. Equation 9 can be further simplified, by using the numerical values of $\sigma_P/\sigma_{Au} = 1.192/9.58$ (tabulated values)[43] and $L_P^Q/L_{Au}^Q = 3.86/1.745$ (Table 4). If we introduce the notation $X_P = I_P/I_{Au}$ for the experimental P/Au intensity ratio and $R_{Au} = I_{Au}/I_{Au}^0 = \exp(-t/L)$ for the attenuation of the Au signal (see eq 1), we obtain

$$X_P \approx 0.28 \frac{N_P}{N_{Au}} \frac{1 - R_{Au}}{R_{Au}} \tag{10}$$

The P/Au *relative atomic density* is approximately independent of the thickness of the DNA film with an average experimental value $N_P/N_{Au} = 0.032$ (Tables 5 and 6), so the Au attenuation factor can be approximated as

$$R_{Au} \approx \frac{1}{1 + 112X_P} \tag{11}$$

Because R_{Au} and X_P are both just ratios of measured peak intensities, the functional dependence between the two can be determined without any assumptions about the coverage or film structure (Figure 6). Equation 11 may be the closest to a parameter-free representation of the signal attenuation available for this system. As shown in Figure 6, the results are well described by eq 11, providing additional evidence that the simple exponential attenuation model is valid for DNA films on Au. Note that eq 11 should be generally applicable for approximate interpolation and extrapolation of XPS data for samples with similar films.

Perhaps the most convincing way to validate our XPS analysis methodology is to directly compare the results with coverages determined independently by a different method. We have complementary FTIR data (Figure 7) for these DNA films where signal attenuation is not a factor in the coverage determination because absolute values of absorbance are ≤1 × 10^{-3}. The two carbonyl bonds of the thymine ring (Figure 1) produce a strong stand-alone peak at 1714 cm^{-1} in the FTIR spectra.[8,61] In general, coverage determination by integration of FTIR absorbance peaks is not reliable because of the possible orientation effects in the FTIR signal. However, if the film is thick and disordered or if the ordering and the dynamic dipole moments do not change throughout a series of samples, FTIR can be used for quantitative coverage measurements. Because the peak at 1714 cm^{-1} in the FTIR data corresponds to free thymine rings,[8] in a comparison with XPS data the chemisorbed components (the two lower BE N 1s components in Figure 2) must be excluded from the coverage analysis. Figure 8 shows a comparison of the DNA coverage determined by FTIR (integrated peak area between 1615 and 1800 cm^{-1}, Figure 7) and from the main N 1s component[62] of the XPS spectra (400.5−401.0 eV BE in Figure 2). *There is an almost perfect linear correlation between the two measurements*. Given the completely different physics of the two techniques, the correlation provides strong support for the validity of two important assumptions: that the average orientation of the thymine rings in the film does not change (so the intensity of the carbonyl stretch in FTIR is proportional to coverage) and that the simple overlayer−substrate model is generally appropriate for the XPS analysis.

(60) Laibinis, P. E.; Bain, C. D.; Whitesides, G. M. *J. Phys. Chem.* **1991**, *95*, 7017−7021.

(61) Haiss, W.; Roelfs, B.; Port, S. N.; Bunge, E.; Baumgartel, H.; Nichols, R. J. *J. Electroanal. Chem.* **1998**, *454*, 107−113.

(62) For example, for the 1 min sample the relative coverage from total N 1s intensity is 0.086/0.313 = 0.27 (Table 6, Figure 5). The intensity of the main N 1s components is 0.95 and 0.71 of the total for the 1200 and 1 min samples, respectively (Table 1); thus the relative coverage based on the main N 1s component only becomes 0.27 × 0.71/0.95 = 0.20 as shown in Figure 8.

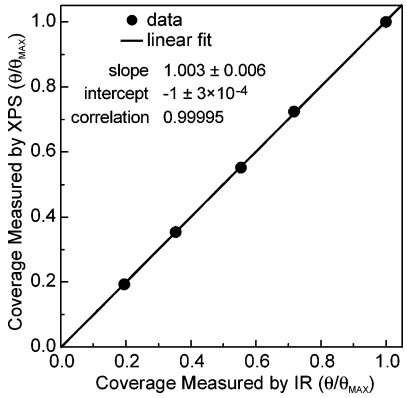

Figure 8. Comparison of the $(dT)_{25}$−SH ssDNA coverage calculated from XPS and FTIR data (normalized to the respective maxima). Only the peaks associated with nonchemisorbed thymine are included [i.e., N 1s between 400.5 and 401.0 eV (Figure 2) and ν(C═O) at 1714 cm^{-1} (Figure 7)] in the calculations. The linear fit (solid line) demonstrates a nearly perfect linear correlation between the coverage values obtained from the two techniques.

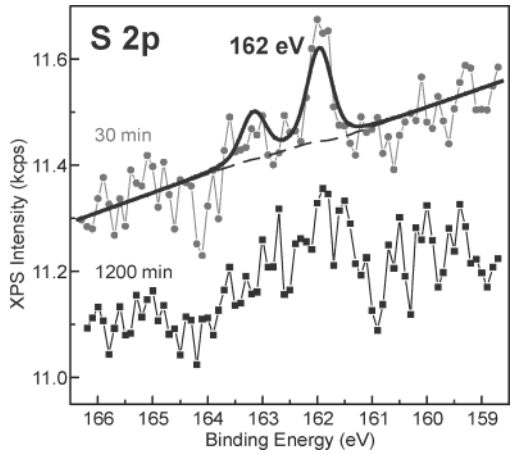

Figure 9. XPS spectra for the S 2p region for samples after 30 and 1200 min of immobilization (1 μM $(dT)_{25}$−SH in 1 M K_2HPO_4−TE buffer). The 30 min sample (gray circles and line) exhibited the strongest S 2p signal in the series. A tentative fit shown by the thick solid line (dashed line background) indicates a 162 eV BE for the S $2p_{3/2}$ component. Both the signal and signal-to-noise are reduced for the 1200 min sample (black squares and line). Note that peaks in the 163−164 eV BE region, characteristic of unbound thiols, are not observed for either sample.

Sulfur Signal: Thiol-Gold Bonding and Coverage. For the thiol-modified ssDNA probes used in our experiment, the sulfur signal in XPS is of interest because it provides information about the degree to which the DNA is covalently immobilized versus nonspecifically adsorbed.[32] The S 2p signal, however, is extremely difficult to observe for these $(dT)_{25}$−SH films because of the very low relative concentration of S (the ideal S/P ratio is 1/25) and the strong attenuation by the DNA film. In fact, the extremely weak S signal intrinsically suggests that S atoms are located at the DNA/Au interface, as expected. The cleanest S 2p spectrum was observed for the sample after the 30 min immobilization (Figure 9). A fit indicates the S $2p_{3/2}$ peak position to be at a BE of 162 eV. This BE is in excellent agreement with values attributed to a thiolate S−Au bond in alkanethiol SAMs.[18−21] Notably, there is no intensity in the 163−164 eV BE range that is typical for a S 2p doublet of unbound thiol groups.[18−22] These two observations strongly suggest that a single layer of the $(dT)_{25}$−SH molecules is chemisorbed via a thiol−gold bond at the surface. In addition, $(dT)_{25}$−SH molecules in a multilayer (i.e., a physisorbed) film would produce a significant unbound thiol signal that would increase for high-coverage films, an effect not observed.

Because the sulfur atoms are bound to the Au at the bottom of the DNA film, the S 2p/Au 4f intensity ratio can be used directly to estimate the S coverage (any attenuation should be essentially the same for both elements). From the fit in Figure 9, this ratio is 8×10^{-4}. This result can be compared to a value of 64×10^{-4} reported[23] for a full SAM of octanethiol on Au(111) with a density of 4.6×10^{14} molecules/cm^2, indicating a S coverage of $(6 \pm 3) \times 10^{13}$ atoms/cm^2. Although this coverage is higher than the 2.3×10^{13} molecules/cm^2 DNA coverage calculated for this sample (Table 6 and Figure 5a), the discrepancy is not significant given the uncertainty of the S coverage associated with the poor signal-to-noise in the S 2p spectrum. In fact, if S-$(CH_2)_6$OH groups from disulfide-protected linkers remain on the surface, S coverage can be up to twice as high as DNA molecular coverage. A potential additional source of a systematic uncertainty is that the Au signal from our polycrystalline substrates will probably be different from that of the Au(111) surface used in ref 23.

Uncertainty Budget

A rigorous, formal analysis of the complete uncertainty budget for our characterization method is beyond the scope of this paper. However, our consideration of the main contributions to the uncertainty, presented in Validation section, indicates that quantitative analysis can be carried out for this system with a high degree of confidence, as expected for XPS applications with thin bio-organic films.[13,14,63] The main random contributions to the uncertainty come from statistical scatter of the data and from instrumental factors, each estimated to be between 5% and 10%. The uncertainty contribution from parameters of the DNA film is strongly suppressed in derived relative coverages and elemental concentrations. The combined *random* uncertainty of values for the *relative* coverages and concentrations is estimated to be between 15% and 20%.

In addition, the *absolute* coverage measurements are subject to a *systematic* uncertainty contributed by the ratio L^Q_{Au}/L^Q_N of the QEALs for Au 4f photoelectrons in Au and for N 1s photoelectrons in the DNA film (eq 4). Both values are calculated using the SRD-82 software.[40] The value of L^Q_{Au} is derived from the recommended IMFPs[40] for Au 4f electrons in gold, which have an uncertainty estimated by the software developers to be ≈10%.[40] We also note that a systematic difference between the calculated and measured values of the IMFP for Au has been previously reported and attributed to surface effects.[64,65] The L^Q_N QEAL for N 1s photoelectrons in the DNA film had to be calculated using experimental parameters for the DNA film (as described in DNA Film Parameters section). The uncertainty for the absolute value of this QEAL is given by the software developers as ≈20%.[40] The contribution from the uncertainty in the DNA film parameters is somewhat alleviated because L^Q_N appears in a ratio to the film thickness (see eq 7 and Invariant EAL Ratios section).

(63) Ratner, B. D.; Castner, D. G. In *Surface Analysis*: *The Principal Techniques*; Vickerman, J. C., Ed.; Wiley: Chichester, U.K., 1997; pp 43−98.
(64) Powell, C. J.; Jablonski, A. *J. Vac. Sci. Technol., A* **1999**, *17*, 1122−1126.
(65) Powell, C. J.; Jablonski, A. *J. Phys. Chem. Ref. Data* **1999**, *28*, 19−62.

Another source of systematic uncertainty in the absolute coverage values is the assumptions of ideal DNA film stoichiometry and of the bulk Au density for vacuum-deposited polycrystalline Au films, both used to obtain the conversion factors in eq 6 and Tables 5−7. The primary effect of all the above systematic uncertainties is an overall shift of the calculated coverage values by a constant factor. This systematic uncertainty can be potentially eliminated by calibration of the absolute coverage against an accurate quantitative method such as radiolabeling. Note that this systematic uncertainty *does not* affect any functional dependence that can be inferred from the calculated coverage values (e.g., versus immobilization time).

Conclusions

We have described how to use XPS to accurately characterize DNA immobilized on gold substrates. Our characterization was performed with immobilized $(dT)_{25}$−SH, a model film with properties that make it useful for validating the applicability of surface characterization methods to DNA films. Using this model system, we have established and validated a methodology for quantitative measurements of the relative and absolute molecular coverages of DNA films immobilized on gold surfaces. The results of the XPS analysis show excellent agreement with FTIR and radiolabeling data for this model system and other related systems. We have thoroughly explored the DNA film parameters used for EAL calculations within the TPP-2M framework and suggested a self-consistent approach for their determination for DNA samples. We estimate the overall *random uncertainty* of our analysis method to be between 15% and 20%. An additional *systematic uncertainty* may result in a simple shift of the calculated *absolute coverage* values by a constant factor but could be eliminated by calibration against an accurate method such as radiolabeling. Because our analysis procedure relies on a minimal set of assumptions that are typically satisfied for biological films, this procedure can be readily generalized to other DNA films (including those with diluent thiols or biocompatible polymers) and biomolecular films including proteins.

Acknowledgment. This work made extensive use of and was greatly facilitated by the NIST SRD-82 EAL database software and the accompanying model, for which the authors thank Drs. Powell and Jablonski. D.Y.P. thanks Dr. Cedric Powell (NIST) for enlightening discussions of the electron attenuation length formalism and careful reading of the manuscript, Dr. Noel Turner (NRL) for his assistance with the XPS setup and helpful suggestions on quantitative XPS analysis, Dr. Max Lagally (UW−Madison) for lecture notes and a formal introduction to quantitative surface analysis, Dr. Franz Himpsel (UW−Madison) for suggestions and advice on photoelectron spectroscopy, and Drs. George Schatz and Mark Ratner (Northwestern) for discussions of DNA film properties. Work at NRL was supported by the Office of Naval Research and the Air Force Office of Scientific Research.

Appendix: Analyzer Binding Energy Calibration

The analyzer binding energy scale was originally set by the manufacturer based on measurements of Au, Ag, and Cu reference samples. To check for any changes in the BE calibration, we compared the positions of Au $4f_{7/2}$ and Au $4d_{5/2}$ peaks measured by this instrument for Au polycrystalline films cleaned by Ar ion sputtering. The comparison included four Au samples prepared in the same way as the Au substrates in this study. The samples were measured on four separate occasions over a period of about a month, using identical instrument settings.

We used two methods to determine the peak positions from the data for the above four sets.[66,67] In the first method, the peak positions were determined from parameters of fits to data using commercial XPS analysis software.[24,26] Au $4f_{7/2}$ and Au $4d_{5/2}$ peaks were fit using a convolution of Gaussian and Lorentzian for line shapes and Shirley function for backgrounds. Fit parameters have not been restricted but converged to consistent values for the four samples. In the second method, we fit a Gaussian function to the top 15% of a peak and used the position of the Gaussian to determine the peak position.[67]

The resulting average values and standard deviations were as follows. Method 1: BE(Au $4f_{7/2}$) = (84.038 ± 0.014) eV, BE(Au $4d_{5/2}$) = (335.16 ± 0.02) eV. Method 2: BE(Au $4f_{7/2}$) = (84.060 ± 0.015) eV, BE(Au $4d_{5/2}$) = (335.282 ± 0.026) eV. The standard accepted values are BE(Au $4f_{7/2}$) = (83.98 ± 0.02) eV[68] and BE(Au $4d_{5/2}$) = 335.22 eV,[69] respectively. For Au 4d peaks, the peak to inelastic background ratio is lower than for Au 4f. Method 1 takes the background into account, whereas Method 2 does not, which accounts for the discrepancy between the two measured values for Au 4d.

Independent of the method used, however, the measured BEs of the Au $4f_{7/2}$ and Au $4d_{5/2}$ peaks differ from the standard values by less than 0.1 eV, which suggests that within the precision used to quote the BE values in this work, no recalibration is necessary. Note that the value of 83.9 eV reported earlier[8] for the Au $4f_{7/2}$ BE from this data set was based on a simultaneous fit to both peaks in the Au 4f doublet and their background, which is subject to greater uncertainty than the two above methods; thus no readjustment of the previously reported BE for elements in DNA films is necessary. The most significant factor that determines the uncertainty of the peak BE reported here for the elements in DNA films (e.g., Table 1) is thus not the analyzer energy calibration but the shifts due to extra-atomic processes, which may differ when different X-ray sources, acquisition conditions, or film preparation conditions are used.

LA034944O

(66) Powell, C. J. *Surf. Interface Anal.* **1995**, *23*, 121−132.
(67) Powell, C. J. *Surf. Interface Anal.* **1997**, *25*, 777−787.
(68) Seah, M. P. *Surf. Interface Anal.* **1989**, *14*, 488−488.
(69) Powell, C. J. *Appl. Surf. Sci.* **1995**, *89*, 141−149.